




Article

Sensing Magnetic Field and Intermolecular Interactions in Diamagnetic Solution Using Residual Dipolar Couplings of Zephycandidine

Radosław M. Kowalczyk ^{1,*} , Patrick J. Murphy ² and Jamie Tibble-Howlings ²

¹ Chemical Analysis Facility, School of Chemistry, Food and Pharmacy, University of Reading, Whiteknights Campus, P.O. Box 224, Reading RG6 6AD, UK

² School of Natural Sciences (Chemistry), Bangor University, Bangor LL57 2UW, UK

* Correspondence: r.m.kowalczyk@reading.ac.uk

Abstract: An unusual residual dipolar coupling of methylene protons was recorded in NMR spectra because aromatic zephycandidine has preferential orientation at the external magnetic field. The observed splitting contains contribution from the dipole–dipole D -coupling and the anisotropic component of J -coupling. Absolute values of the anisotropy of magnetic susceptibility $|\Delta\chi_{ax}|$ are larger for protic solvents because of the hydrogen-bonding compared to aprotic solvents for which polar and dispersion forces are more important. The energy barrier for the reorientation due to hydrogen-bonding is 1.22 kJ/mol in methanol- d_4 , 0.85 kJ/mol in ethanol- d_6 and 0.87 kJ/mol in acetic acid- d_6 . In dimethyl sulfoxide- d_6 , 1.08 kJ/mol corresponds to the interaction of solvent lone pair electrons with π -electrons of zephycandidine. This energy barrier decreases for acetone- d_6 which has smaller electric dipole moment. In acetonitrile- d_3 , there is no energy barrier which suggests solvent ordering around the solute due to the solvent-solvent interactions. The largest absolute values of the magnetic anisotropy are observed for aromatic benzene- d_6 and toluene- d_8 which have their own preferential orientation and enhance the order in the solution. The magnetic anisotropy of “isolated” zephycandidine, not hindered by intermolecular interaction could be estimated from the correlation between $\Delta\chi_{ax}$ and cohesion energy density.

Keywords: residual dipolar couplings (rdc); Nuclear Magnetic Resonance (NMR); zephycandidine; magnetic anisotropy; magnetic susceptibility; aromatic molecule; cohesive energy density (ced)



Citation: Kowalczyk, R.M.; Murphy, P.J.; Tibble-Howlings, J. Sensing Magnetic Field and Intermolecular Interactions in Diamagnetic Solution Using Residual Dipolar Couplings of Zephycandidine. *Int. J. Mol. Sci.* **2022**, *23*, 15118. <https://doi.org/10.3390/ijms232315118>

Academic Editors: Mateusz Reczyński and Szymon Choraży

Received: 14 November 2022

Accepted: 25 November 2022

Published: 1 December 2022

Publisher’s Note: MDPI stays neutral with regard to jurisdictional claims in published maps and institutional affiliations.



Copyright: © 2022 by the authors. Licensee MDPI, Basel, Switzerland. This article is an open access article distributed under the terms and conditions of the Creative Commons Attribution (CC BY) license (<https://creativecommons.org/licenses/by/4.0/>).

1. Introduction

Residual dipolar couplings (rdc) have become an important tool in elucidating structure and conformation of macromolecules [1–4]. They arise because of a direct interaction between nuclear magnetic moments and are observed in solution-state Nuclear Magnetic Resonance (NMR) spectra when free motion of molecules is restricted [5,6]. That is usually achieved by using a diamagnetic medium (such as liquid crystal or polymer gel) with ability to introduce the preferential orientation of solute molecules [1–4,7–9]. Anisotropic interactions are no longer fully averaged in such solution, and they could be experimentally detected and analyzed using Saupe formalism of an alignment tensor and resulting ordering parameter [10–12].

Diamagnetic aromatic molecules possess a unique ability to orient themselves spontaneously in the solution in the presence of the external magnetic field without a need for the orientating medium [13–17]. This effect is dependent on the anisotropy of the molecule magnetic susceptibility and is relatively rarely observed experimentally, as the strength of the dipole–dipole interaction depends on the inverse cube of the distance [18–20]. Exceptionally stable conditions for a solution-state NMR experiments are required to observe a small dipolar splitting of resonances in the spectrum which are in the order of 1 Hz at the highest achievable magnetic fields (~23 T) for commercially available spectrometers [16].

Those difficulties limit the potential use of the residual dipolar couplings to explore the magnetic properties of diamagnetic aromatic molecules in various diamagnetic solvents. In particular, intermolecular interactions between solvent and solute could provide valuable experimental insight into how the isolated diamagnetic molecule senses its environment, how effectively the diamagnetic solvent shields the solute from the external magnetic field and how it controls the molecular dynamic of the solution [21].

In this contribution, the rare residual dipolar couplings between methylene protons of zephycandidine at magnetic fields of 16.445, 11.440, 9.390 T are reported. Combination of a large magnetic anisotropy of this diamagnetic aromatic molecule and proximity of interacting magnetic moments results in the large splitting (~ 0.6 Hz) of the resonance line in NMR spectra. This allows elucidation, with significant precision, the effect of the diamagnetic surrounding of the solvent on the magnetic anisotropy of the solute molecule for several deuterated solvents and at the wide range of temperatures. The experimentally estimated magnetic anisotropy clearly depends on the ability of the solvent to suppress fast reorientation dynamic of the solute. Zephycandidine molecule requires additional energy to change its preferential orientation in solvents with the ability to form strong hydrogen-bonds and such additional energy barrier has been observed and estimated for methanol- d_4 , ethanol- d_6 and acetic acid- d_4 . Dispersion and polar forces dominate interactions for aprotic solvents used. The energy barrier related to the interaction of solvent lone pair electrons with π -electrons of zephycandidine is mediated by the electrostatic forces in dimethyl sulfoxide- d_6 and it is comparable to the energy barrier estimated for hydrogen-bonding. The importance of the molecular dynamic in the solvent-solute system is also confirmed by data which clearly show substantial enhancement of the magnetic anisotropy of zephycandidine dissolved in the aromatic benzene- d_6 and toluene- d_8 which have ability to self-order at the external magnetic field.

This contribution demonstrates also a unique experimental concept how the geometry of zephycandidine combined with two independent sources of information about its magnetic anisotropy could be used to distinguish between the direct dipole–dipole D -coupling and the anisotropic component of indirect J -coupling.

This study, for the first time, correlates the magnetic anisotropy of the solute with the experimentally measured cohesion energy density of the solvent. As a result, the anisotropy of the magnetic susceptibility for the solute molecule which does not experience any hindrance for the reorientation in the solution could be estimated.

2. Results and Discussion

The ^1H NMR spectrum of zephycandidine dissolved in methanol- d_4 recorded at 16.445 T (700 MHz spectrometer) is shown in Figure 1. The assignment of all resonances to the molecular structure agrees fully with previously published data [22–24].

The resonance at 6.155 ppm shows a splitting of 0.631 Hz which is not expected in solution unless the symmetrical position of methylene protons in the molecule is distorted [25,26] or the motion of the solute is no longer isotropic [13–17]. Experimental conditions must be excluded as a possible source of this splitting because tetramethylsilane (TMS) forms a symmetric Lorentzian-shape resonance [27] with a half-amplitude width of ca. 0.5 Hz (Figure 1). There is also no evidence of any systematic distortions to other resonances in the spectrum (Figure 1). Deviations from the symmetrical position of methylene protons in aromatic zephycandidine could produce inequivalence in the chemical shift, and hence the splitting but would be observed uniformly at both low and high magnetic fields [25,26]. Similarly, an unlikely contribution from the isotropic J -coupling would not change between low and high magnetic fields [28,29]. In contrast, the observed splitting decreases to 0.316 Hz at 11.440 T and to 0.209 Hz at 9.390 T as shown in the inset of Figure 1. Therefore, the primary origin of the observed splitting is the anisotropic direct dipole–dipole interaction reintroduced to the NMR spectrum by a partial orientation of solute molecules in the solution [13–17].

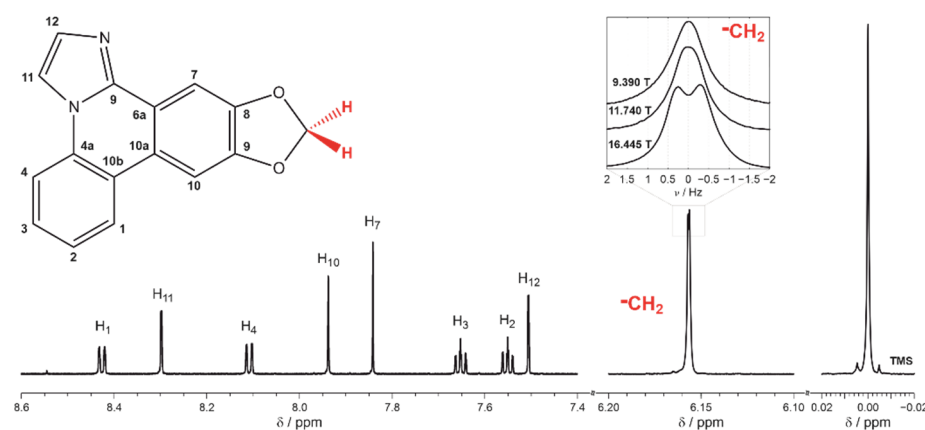


Figure 1. The assignment of ^1H resonances to the molecular structure of zephycandidine. The methanol- d_4 solution spectrum was recorded at 16.445 T using 700 MHz spectrometer. The inset compares the resonance of methylene protons observed at 16.445, 11.740 and 9.380 T recorded using 700, 500 and 400 MHz NMR instruments, respectively.

Similar results have been obtained for zephycandidine dissolved in several various solvents. Figure 2 shows in more detail, the magnetic field dependence of the splitting for dimethyl sulfoxide- d_6 , acetone- d_6 , and chloroform- d . The additional point was added to the experimental results because any anisotropic component must be equal zero at zero magnetic field ($B_0 = 0$ T) and in the absence of the isotropic J -coupling, in accordance with the quadratic dependence on the external magnetic field B_0 (see Section 3.1 and [18–20] for more information). The consistency of the results between various solvents confirms that the experimental conditions or solution preparation are not responsible for the observed splitting because it is highly unlikely for them to influence each investigated sample in the same manner.

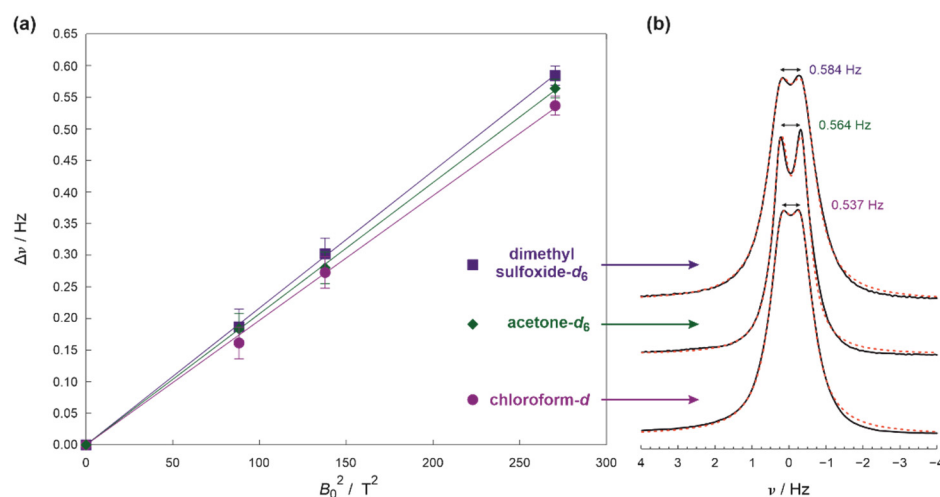


Figure 2. (a) The magnetic field dependence of the methylene resonance splitting for zephycandidine dissolved in dimethyl sulfoxide- d_6 , acetone- d_6 and chloroform- d . (b) The methylene resonances (solid black lines) and their simulations (red dotted lines) for these solvents recorded using 700 MHz spectrometer at 16.445 T.

The final piece of evidence that the observed splitting of the methylene resonance is caused by anisotropic dipolar interaction is shown in Figure 3(b–b’). This figure presents the magnetic field dependence of the splitting for the resonances which originate from the protons laying in the plane of the molecule. It is clear, that all values increase on decreasing the B_0 , which is consistent with the presence of both anisotropic dipolar D (dependent on

B_0) and isotropic indirect J_{iso} (independent from B_0) components to the splitting $\Delta\nu$ (see Section 3.1 and [18–20] for more detailed information).

The observed splitting of the methylene resonance is among the largest observed experimentally because of the proximity of the interacting protons (ca. 1.81 Å) and uniquely its value could be measured directly in the spectrum (e.g., without a need to analyze the differences in J -couplings as show in Figure 3(a–a’’) for other protons) [19]. This experimental advantage combined with a well-defined molecular geometry of zephycandidine allow to elucidate the anisotropy of the magnetic susceptibility ($\Delta\chi_{ax}$) using simplified Equation (2) as described in Sections 3.1 and 3.3 and is presented in Figure 2a. Values of $\Delta\chi_{ax}$ obtained for various solvents in which zephycandidine fully dissolves are collected in Table 1. The same table also lists the anisotropy $\Delta\chi_{ax}$ and rhombicity $\Delta\chi_{rh}$ of the magnetic susceptibility estimated in the more conventional way by analyzing J -couplings for three- and four-bonds distant protons in the plane of the molecule. The mathematical details of the utilized Equation (4) are given in Sections 3.1 and 3.3. Figure 3a–a’’ shows in detail the resonances selected, and the representative result is presented in Figure 3c. The detailed structural parameters used to estimate $\Delta\chi_{ax}$ and $\Delta\chi_{rh}$ in the second method are given in Table 2 in Section 3.3.

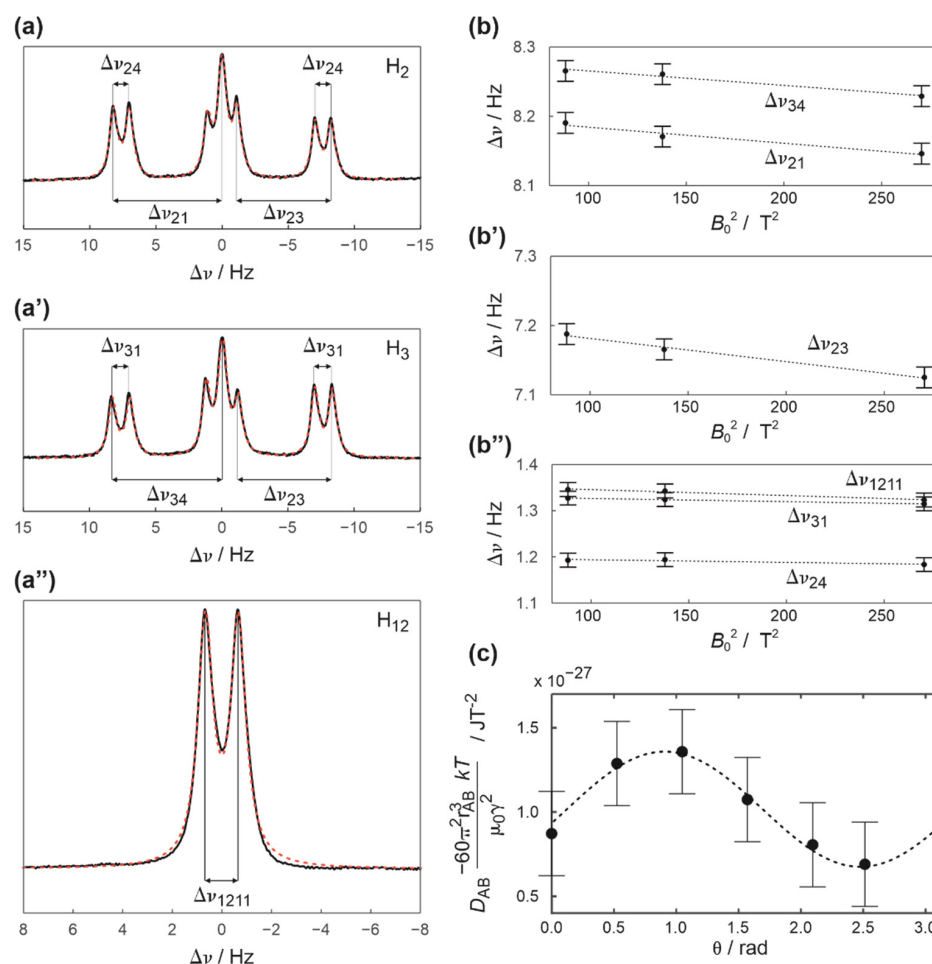


Figure 3. (a–a’’) The resonances of H₂, H₃ and H₁₂ protons (solid black lines) and their simulations (red dotted lines) obtained for zephycandidine dissolved in tetrahydrofuran-*d*₈ at 16.445 T using 700 MHz NMR spectrometer. The index to splitting $\Delta\nu$ corresponds to the numbering of interacting protons. (b–b’’) The magnetic field dependence of $\Delta\nu$ used to extract corresponding values of D . (c) The angular dependence of the normalized values of D as detailed in Equation (4) in Section 3.3 used to estimate magnetic anisotropy parameters $\Delta\chi_{ax}$ and $\Delta\chi_{rh}$. The structural details used are listed in Table 2.

Table 1. The anisotropies $\Delta\chi_{ax}$ and rhombicities $\Delta\chi_{rh}$ of the magnetic susceptibility calculated for zephycandidine dissolved in various solvents and estimated from the residual dipolar couplings of methylene protons (column 3) and in-molecular-plane protons (column 4 and 5). The estimated energy barriers ΔE for the reorientation of zephycandidine due to intermolecular interactions are listed in column 6. The experimental errors are given below each column.

Solvent		$\Delta\chi_{ax}/\text{JT}^{-2}$	$\Delta\chi_{ax}/\text{JT}^{-2}$	$\Delta\chi_{rh}/\text{JT}^{-2}$	$\Delta E/\text{kJ/mol}$
aromatic	benzene- d_6	-1.86×10^{-27}	-1.41×10^{-27}	-0.35×10^{-27}	0.00
	toluene- d_8	-1.91×10^{-27}	-1.51×10^{-27}	-0.57×10^{-27}	0.13
protic	acetic acid- d_6	-1.79×10^{-27}	-1.33×10^{-27}	-0.41×10^{-27}	0.87
	methanol- d_4	-1.80×10^{-27}	-1.32×10^{-27}	-0.28×10^{-27}	1.22
	ethanol- d_6	-1.66×10^{-27}	-1.21×10^{-27}	-0.29×10^{-27}	0.85
aprotic	dimethyl sulfoxide- d_6	-1.64×10^{-27}	-1.21×10^{-27}	-0.63×10^{-27}	1.08
	acetone- d_6	-1.60×10^{-27}	-1.16×10^{-27}	-0.38×10^{-27}	0.33
	tetrahydrofuran- d_8	-1.57×10^{-27}	-1.01×10^{-27}	-0.21×10^{-27}	0.13
	acetonitrile- d_3	-1.53×10^{-27}	-1.01×10^{-27}	-0.23×10^{-27}	0.05
	chloroform- d	-1.52×10^{-27}	-1.00×10^{-27}	-0.27×10^{-27}	0.02
standard errors (confidence level 95.4%)		0.06×10^{-27}	0.14×10^{-27}	0.12×10^{-27}	0.28

There are differences between $\Delta\chi_{ax}$ estimated using both methods with the second method consistently underestimating the value of $\Delta\chi_{ax}$ by ca. 30% (Table 1). There are a few possible reasons which could explain this difference, which is larger than the sum of the experimental errors (see Section 3.3 for details). Firstly, it is possible that the internuclear vector \mathbf{r}_{AA} (between the methylene protons) is not parallel to the main component of the magnetic susceptibility tensor χ . However, the tilt of \mathbf{r}_{AA} in reference to χ_{zz} direction should be in the order of ca. 20 degree to account fully for the observed difference. Such tilt is extremely unlikely for a molecule such as zephycandidine because of the geometry of methylene site, axial symmetry, and aromatic character [19,30]. It would also be expected that any deviation from the zero-degree angle would induce an imbalance in the magnetic shielding of the methylene protons and evidence of this should be visible in the NMR spectra consistently at all magnetic fields [25,26]. Secondly, it is necessary to consider that the \mathbf{r}_{AB} (between the protons in the plane of the molecule) is not perpendicular to χ_{zz} direction. Again, only tilt of ca. 45 degree would account for the whole difference, and it is rather unlikely that such large distortion is possible [19,30]. The third possibly assumes the presence of the anisotropy of the indirect J -coupling. J_{aniso} would follow similar dependence on $\Delta\chi_{ax}$ and the external magnetic field B_0 as the direct D -coupling via its dependence on ordering parameter but has been omitted in the evaluation of mathematical equations (see Section 3.1) because its value is usually negligible for light-nuclei such as protons [31]. Further work would be required to improve experimental data (specially to increase number of magnetic field points), together with detailed calculation to provide more definitive, quantitative conclusion which would separate both contribution to the experimental $\Delta\nu$. However, it is interesting to point out that according to theory, J_{aniso} at the most favorable conditions may contribute up to 30% to the experimentally estimated value of D [20].

It is likely that all three factors play some role in the observed difference. However, it is necessary to assume that the J_{aniso} is the most significant and therefore, the experimentally measured splitting $\Delta\nu$ of the methylene resonance should be regarded as “effective” value containing both contributions.

The estimated values of rhombicities $\Delta\chi_{rh}$ estimated from the J -coupling splitting for three- and four-bonds distant protons in the plane of the molecule are also listed in Table 1. Unfortunately, significant experimental errors prevent any in-depth analysis beyond the qualitative conclusion that they are about two-to-four times smaller than $\Delta\chi_{ax}$ estimated in the same procedure for various solvents. That intuitively agrees with the fact that the zephycandidine in-plane structure deviates from a circular geometry and has a more oval elongated shape (see Figure 1) [32].

The experimentally estimated $\Delta\chi_{ax}$ are about double the values reported for benzene [16,20] and vary between the solvents with the largest absolute values calculated for aromatic solvents such as toluene- d_8 and benzene- d_6 and the smallest obtained for an aprotic acetonitrile- d_3 and chloroform- d (Table 1). Magnetic anisotropies calculated from $\Delta\nu$ of methylene protons have significantly better precision (smaller experimental errors) and only these values are considered in the discussion below.

To understand the differences in $\Delta\chi_{ax}$ between solvents, it is necessary to re-examine their role in establishing conditions for the NMR experiments. Figure 4 shows the magnetic anisotropies $\Delta\chi_{ax}$ plotted as a function of the cohesion energy density (ced) normalized to the relative magnetic permeability μ_{sol} of the solvent. More details describing the selection of these experimentally measured parameters from previously published data are given in Section 3.4 and Supplementary Material.

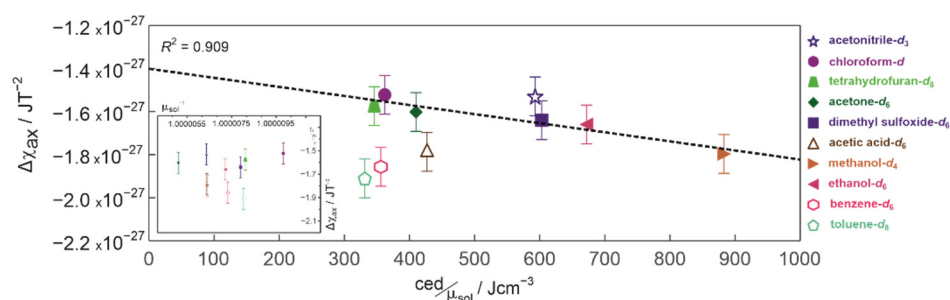


Figure 4. The magnetic anisotropy $\Delta\chi_{ax}$ of zephycandidine plotted as a function of the cohesion energy density normalized to the solvent relative permeability. The dotted line represents a linear regression fit to experimental data presented by filled symbols. The inset shows $\Delta\chi_{ax}$ as a function of the inverse of magnetic permeability.

The choice of ced and permeability is related to two major impacts diamagnetic solvent has on the solute molecule: the control of its molecular dynamic and shielding it from the external magnetic field B_0 . The ced (equal to energy per molar volume) describes the amount of energy needed to break solvent into separate non-interacting molecules, and intuitively provides information how difficult is to re-arrange molecules in the solvent [33,34]. Such information is relevant because zephycandidine to orient itself in the magnetic field needs to work against the forces which hold solvent together and these exact forces would also help zephycandidine to stay at the preferential orientation before the thermal energy destroys a fragile momentary equilibrium. Relative permeability is very closely related to the volume magnetic susceptibility, i.e., $\mu_{\text{sol}} = 1 + \chi_{\text{sol}}$. Magnetic susceptibility has been proven to have a measurable influence on the spectral parameters such as chemical shift and linewidth, and depends on the sample quality, geometry, environment, and temperature [35–38]. Diamagnetic solvents have a relative magnetic permeability that is less than or equal to one and therefore, the effective magnetic field B_{eff} experienced by the solute is usually smaller than the external magnetic field B_0 .

Excluding aromatic benzene- d_6 and toluene- d_8 which special case will be discussed later, it is clear from Figure 4, that the absolute values of the magnetic anisotropy $|\Delta\chi_{ax}|$ increase with the increase in the $\text{ced}/\mu_{\text{sol}}$ ratio. This suggests that the main reason for the observed differences is the increase in the average time zephycandidine spends at the preferential orientation because the larger the $\text{ced}/\mu_{\text{sol}}$ ratio the more energy required to re-arrange the momentary equilibrium in the solution. This is consistent with the principle of each NMR experiment which provide a snapshot of a time averaged equilibrium and the observation that the magnetic susceptibility could not be a major factor responsible for observed differences because $\Delta\chi_{ax}$ scatter randomly as function of $1/\mu_{\text{sol}}$ (see inset in Figure 4). The absence of any clear correlation in the inset of Figure 4, also indirectly proves that the experimental error sufficiently accounts for any differences related to the solutions quality and the finite volume and shape of NMR tube between investigated samples.

Despite a clear correlation between $\Delta\chi_{ax}$ and $\text{ced}/\mu_{\text{sol}}$, there are two possible inconsistencies: (i) relatively small $\text{ced}/\mu_{\text{sol}}$ ratio in the case of acetic acid- d_6 compared to other protic solvents and (ii) unexpectedly smaller absolute value of the magnetic anisotropy for aprotic acetonitrile- d_3 compared to other aprotic polar solvents (i.e., dimethyl sulfoxide- d_6 and acetone- d_6) (Figure 4).

The reason for a relatively small $\text{ced}/\mu_{\text{sol}}$ ratio in the case of acetic acid compared to other protic solvents (i.e., methanol and ethanol) could be explained by the underestimated experimental value of ced (427 Jcm^{−3}), taken from reference [39]. The difficulties of evaluating reliable values of ced for carboxylic acids (acetic acid and formic acid in particular) from thermodynamic experiments are well documented and are related to the presence of both monomers and dimers in the gas phase [40–42]. This problem is illustrated in the Supplementary Material Table S3 which compares values of ced estimated for acetic acid in various sources [33,39,43–45]. The ced calculated from early calorimetric studies (enthalpy of vaporization, ΔH_{vap}) ranges from 365 Jcm^{−3} for the evaporation of liquid to the equilibrium mixture of gas at saturation pressure, to 858 Jcm^{−3} for liquid to monomer gas experiment [46]. The molecular dynamic simulations reported in [43], also points towards the larger values 694 and 763 Jcm^{−3} (depending on the simulation procedure) and have a fair agreement with 691 Jcm^{−3} calculated directly from ΔH_{vap} and reported more recently in [47]. This value is closer to these for ethanol (675 Jcm^{−3}) and methanol (874 Jcm^{−3}) [39]. Our data presented in Figure 4, could also provide a crude estimate of the ced from the gradient of the linear correlation between the $\Delta\chi_{ax}$ and $\text{ced}/\mu_{\text{sol}}$. The value of 911 Jcm^{−3} estimated for acetic acid is larger than that of methanol.

To understand better the differences in $\Delta\chi_{ax}$ between solvents and observed inconsistency for acetonitrile- d_3 , it is convenient to consider in more detail molecular level interactions which hold each liquid together. To be able to systematically account for the dispersion and polar forces as well as hydrogen-bonding, the total ced could be divided into three components [33,34,39,48]. This approach has been used successfully to predict efficiency of dissolving chemicals in various solvents by a means of Hansen Solubility Parameters (HSP) [48]. The limitation of this analysis is that individual HSP provide only empirical values because it is impossible to separate and measure directly all these interactions in solution. However, the estimated values of HSP are closely related to the physical properties of the molecule, i.e., dispersion to the refractive index and to the boiling point, polar force to the electric dipole moment, whereas the hydrogen-bonding component could be crudely approximated from spectroscopic data or empirically calculated from a molecular structure or total ced [39,48]. It is necessary to clearly stress that the most significant advantage of this empirical approach is that it provides a uniform tool to compare energies of three major interactions for solvents with distinctive properties, which could not be otherwise measured experimentally in a consistent way.

The effect of polarity on the values of $\Delta\chi_{ax}$ is detailed in Figure 5a. There is a trend (within the experimental error) between $\Delta\chi_{ax}$ and ced^D/ced for aprotic solvents except for acetonitrile- d_3 . The values of $|\Delta\chi_{ax}|$ for dimethyl sulfoxide- d_6 and acetone- d_6 are slightly larger than those for chloroform- d or tetrahydrofuran- d_8 and that coincide with the difference in the electric dipole moment normalized to molar volume (pV_m^{-1}) (Figure 5a). The magnetic anisotropy of zephycandidine in acetonitrile- d_3 is comparable to that for chloroform- d (see also Table 1) despite the pV_m^{-1} ratio being much closer to that of dimethyl sulfoxide- d_6 or acetone- d_6 (Figure 5a and Supplementary Material).

Similar discrepancy for acetonitrile- d_3 could be also seen in Figure 5b which shows $\Delta\chi_{ax}$ plotted versus the ced^D/ced ratios. The $|\Delta\chi_{ax}|$ decreases slightly for solvents with larger ced^D/ced ratio (or smaller $n_D V_m^{-1}$) such as tetrahydrofuran- d_8 and chloroform- d compared to that for dimethyl sulfoxide- d_6 . Such behavior is to be expected because molecules with a large permanent electric dipole will be less sensitive to the presence of weaker dispersive forces but have much greater potential to induce instantaneous dipoles in their environment [49]. That means, that the molecule with the larger permanent electric dipole (i.e., dimethyl sulfoxide- d_6) would have more significant effect on the

zephycandidine, whereas molecules with the larger electric polarizability (and smaller permanent dipoles, i.e., chloroform-*d*) could be more influenced by zephycandidine itself.

The reason for the smaller (in the context described above) value of $|\Delta\chi_{ax}|$ for acetonitrile-*d*₃ compared to other aprotic polar solvents (i.e., dimethyl sulfoxide-*d*₆ and acetone-*d*₆) is not fully clear. However, it is possible to speculate that this inconsistency could be related to acetonitrile molecules being weakly ordered in the solution as observed experimentally by X-ray diffraction, IR spectroscopy [50] and in the DFT calculations [51–54]. This would require any solvent-solvent interactions to dominate and effectively suppress solute-solvent interactions (related to electrostatic forces) and would remove any difficulties for zephycandidine to reorient itself in the solution. This is consistent with a relatively small value of the magnetic anisotropy and the absence of the energy barrier for zephycandidine reorientation in the solution due to the solvent-solute interaction (Table 1, see Section 3.5 and paragraph below). The hydrogen bonding is not expected to play major role for acetonitrile-*d*₃ solution (Figure 5c and Table 1) and the possible error in sample preparation and experimental conditions must be excluded because identical results were obtained for independently prepared samples measured in separated experiments (see Section 3.2).

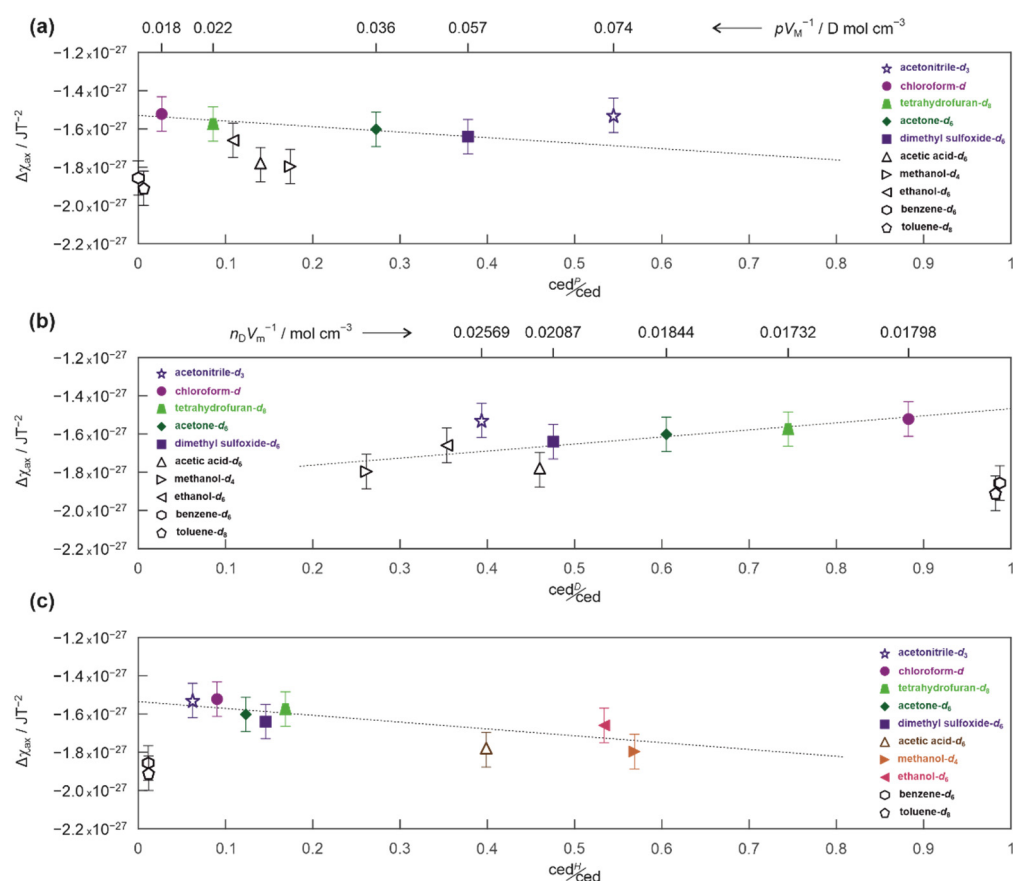


Figure 5. The magnetic anisotropy $\Delta\chi_{ax}$ of zephycandidine plotted as a function of (a) polar, (b) dispersion and (c) hydrogen-bonding components of the total cohesion energy density. The dotted lines are for eye guidance only. The experimental data represented by open symbols are not considered for the guideline in particular graph.

This situation would be different for any solvent which directly and strongly interacts with the solute. It is clear from Figure 6a, that the splitting $\Delta\nu$ in dimethyl sulfoxide-*d*₆ do not follow expected by theory dependence on B_0^2 when compared to that for chloroform-*d* or toluene-*d*₈ and could not be explained by the temperature dependence of the magnetic susceptibility [36–38]. The observed deviation provides a measure of an additional energy which zephycandidine require to reorientation itself in such solution and could be

experimentally estimated from the $\ln(\Delta\nu)$ plots shown in Figure 6b (more details are given in Section 3.5 and Supplementary Material). This additional energy barrier of 1.08 kJ/mol is relatively large, despite dimethyl sulfoxide- d_6 being a proton acceptor which is not expected to form strong hydrogen bonds with zephycandidine (Table 1, Figure 5c). However, its oxygen or sulfur atoms could strongly interact with a π -system of zephycandidine and such anion- π and/or cation- π interactions are mediated by electrostatic forces (Figure 5a,b) [55,56]. It is possible that these anion- π interactions dominate in solution because of the axial symmetry of zephycandidine and the geometry of dimethyl sulfoxide molecule. It could be also speculated that the additional energy barrier should be smaller for molecules with smaller than dimethyl sulfoxide- d_6 electric dipole moment and that is the case for acetone- d_6 with the estimated energy barrier of 0.33 kJ/mol (Table 1).

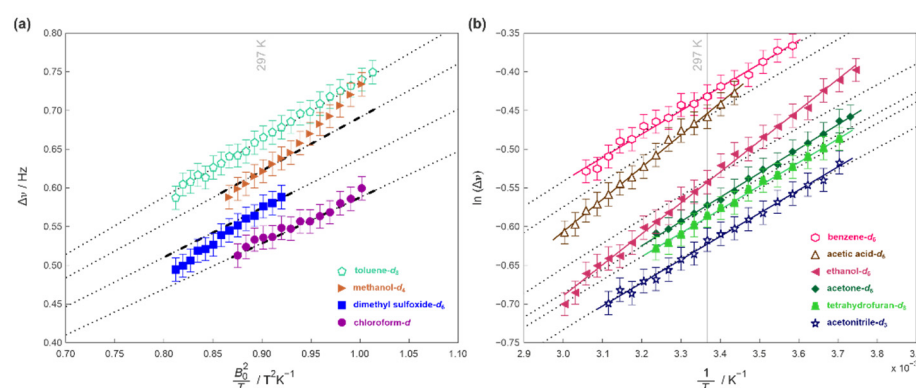


Figure 6. (a) The temperature dependence of the methylene rdc splitting recorded at 16.445 T for zephycandidine in selected solvents. The dotted lines show expected theoretical dependence of $\Delta\nu$ on the temperature and the external magnetic field calculated using Equation (2) for given $\Delta\chi_{ax}$. The bold dash lines show the same theoretical dependence but additionally the temperature variation of the magnetic susceptibility of the solvent was included. (b) The logarithm of $\Delta\nu$ as a function of the temperature. The solid lines were fitted to the experimental data using the Arrhenius equation. The dotted lines represent expected from Equation (2) theoretical dependence of $\ln(\Delta\nu)$ on the temperature.

For protic solvents such as methanol- d_4 and ethanol- d_6 , which are proton donors in hydrogen bonds, the estimated values of ΔE are 1.22, and 0.85 kJ/mol, respectively (Table 1, Figure 6). It is also clear from Table 1 (and Figure 4), that the magnetic anisotropy for protic solvents is larger than for aprotic solvents. The same can be seen in Figure 5c which shows $\Delta\chi_{ax}$ plotted versus ced^H/ced ratio for both protic and aprotic solvents. The correlation between the magnetic anisotropy and the strength of hydrogen-bonding is not surprising. The molecules of zephycandidine are a part of a dynamic system in which constant motions are affected by the presence of external magnetic field B_0 and govern by intermolecular interactions. It is this network of solvent-solute and solvent-solvent hydrogen-bonding which modulates the ability to quickly reorganize the momentary equilibrium, the fingerprint of which is detected in the NMR spectrum [28,29].

It is necessary to point out, that in Figure 5c, the ced^H/ced ratio for acetic acid- d_6 is smaller than that of methanol- d_4 despite nearly identical $\Delta\chi_{ax}$ (Table 1) and acetic acid being a stronger proton donor than methanol. This observation mirrors similar discrepancy observed for the ced determined experimentally from thermodynamic studies (see Figure 4 and discussion above) and suggest that experimental difficulties are related to presence of hydrogen-bonded dimers in the gas phase [40–42,46].

It is clear from Table 1 and Figure 4 that the magnetic anisotropy of zephycandidine in benzene- d_6 and toluene- d_8 has the largest absolute values, despite the evidence of much weaker interactions compared to that present in methanol- d_4 or dimethyl sulfoxide- d_6 . However, that is no surprise considering the aromatic character of these solvents, which molecules have themselves a preferential orientation in the external magnetic field [13,15,16,20]. That is also confirmed by the detection of the quadrupolar splitting

of ^{13}C satellite resonances in their deuterium spectra (Supplementary Material Figure S1). This splitting of ca. 0.574 Hz observed in benzene- d_6 agrees with previously reported data at 23.4 T and follows the expected B_0^2 dependence [16]. There is no significant energy difference for zephycandidine reorientation in neither benzene- d_6 or toluene- d_8 (Figure 6) which confirms that solvent-solute interactions could not cause the increase in the $\Delta\chi_{ax}$ values and the preferential orientation of benzene- d_6 and toluene- d_8 is a main mechanism of the observed enhancement. The extent of this enhancement could be crudely estimated by comparing the experimental value of magnetic anisotropy and the value estimated from the correlation gradient in Figure 4, to be in the order of ca. 15%.

The observed variation in the magnetic anisotropy $\Delta\chi_{ax}$ emerge because of significant differences in the reorientation dynamic of zephycandidine in studied solvents which are caused by solvent-distinctive intermolecular interactions. The $\text{ced}/\mu_{\text{sol}}$ ratio provides an adequate measure for such changes in the molecular dynamics because ced describes how difficult is to re-arrange the molecules and $\mu_{\text{sol}} \approx 1$ for diamagnetic solvents. Therefore, the case when $\text{ced}/\mu_{\text{sol}} = 0$ describes a solute reorientating itself without restrictions imposed by intermolecular interactions with the solvent at unaltered external magnetic field. Considering that, the observed in Figure 4 correlation between $\Delta\chi_{ax}$ and $\text{ced}/\mu_{\text{sol}}$ allows to estimate the anisotropy of magnetic susceptibility for an “isolated” zephycandidine molecule not influenced by the solvent to be approximately $1.41 \times 10^{-27} \text{ JT}^{-2}$.

3. Materials and Methods

3.1. Mathematical Description of Magnetic Field Induced Self-Orientation

Experimentally detected splitting $\Delta\nu$ of the resonance line in NMR spectrum is a sum of a spin-spin J -coupling and dipole–dipole D -coupling and is usually express as: $\Delta\nu = J + 2D$ [20,28,29]. The indirect J -coupling could consist of both isotropic and anisotropic contribution, whereas direct D -coupling has only an anisotropic term which depends on the orientation of the vector \mathbf{r}_{AB} linking interacting magnetic moments in respect to the external magnetic field \mathbf{B}_0 and magnetic susceptibility tensor χ . Using spherical coordinates D could be written as [10–12,19]:

$$D = -\frac{1}{8\pi^2} \frac{\mu_0 \gamma_A \gamma_B}{r_{AB}^3} \frac{B_0^2}{15kT} \left[\Delta\chi_{ax} (3\cos^2\alpha - 1) + \frac{3}{2} \Delta\chi_{rh} (\sin^2\alpha \cos 2\beta) \right] \quad (1)$$

where α is an angle between the vector \mathbf{r}_{AB} linking interacting magnetic moments and the z axis of χ , whereas β identifies position of the \mathbf{r}_{AB} projection onto the xy plane of χ . In Equation (1), two independent parameters: anisotropy $\Delta\chi_{ax}$ and rhombicity $\Delta\chi_{rh}$ of diagonal χ are used and other symbols have their usual meaning [28,29]. For methylene protons in axially symmetric zephycandidine molecule, there should not be any isotropic J contribution to $\Delta\nu$ and a small anisotropic part is neglected as usual in the published literature [20,31]. Further, for planar aromatic molecule such as zephycandidine the principal axis of susceptibility tensor is expected to be normal to the molecule plane [19] and parallel to the \mathbf{r}_{AB} which allows to express experimentally observed splitting as:

$$\Delta\nu = -\frac{1}{4\pi^2} \frac{\mu_0 \gamma^2}{r^3} \frac{B_0^2}{15kT} \Delta\chi_{ax} \quad (2)$$

From this equation, the anisotropy $\Delta\chi_{ax}$ could be estimated, using the magnetic field or temperature dependence of the splitting $\Delta\nu$. In a similar way, for interacting magnetic moments laying in the plane of the molecule (e.g., the \mathbf{r}_{AB} is perpendicular to the principal axis of susceptibility tensor), Equation (1) could be rewritten as:

$$\Delta\nu = J_{iso} - \frac{1}{4\pi^2} \frac{\mu_0 \gamma_A \gamma_B}{r_{AB}^3} \frac{B_0^2}{15kT} \left[\frac{3}{2} \Delta\chi_{rh} \cos 2\beta - \Delta\chi_{ax} \right] \quad (3)$$

allowing for independent evaluation of $\Delta\chi_{ax}$ and $\Delta\chi_{rh}$ which assumes that there is only isotropic contribution of J -coupling to $\Delta\nu$ which does not depend on B_0 [28,29].

3.2. Sample Solutions and NMR Instrumentation

Zephycandidine powder was synthesized as described in [23]. All solutions were prepared by dissolving zephycandidine powder in high quality deuterated solvents purchased from Sigma-Aldrich (level of deuteration > 99.0 %). The final concentration was 0.020(3) % *w/w* to ensure high level of dilution (solute molecules were isolated). Solutions (0.5 mL) were transferred to high-precision NMR tubes with 5 mm outer diameter and kept at ambient/room temperature conditions.

The NMR experiments were carried out at 16.445T, 11.745 and 9.390T which corresponds to 700, 500 and 400 MHz Bruker Avance spectrometer, respectively. 700 MHz spectrometer was equipped with a high-sensitivity TCI cryoprobe, whereas standard BBO probes were used for 500 and 400 MHz instruments. The standard procedure of tuning the probe, locking, and shimming was performed for each sample with a minimum 600 s delay after transfer to the superconducting magnet. Spectra were recorded at constant temperature of 297 K or within a range 273 K–336 K equilibrated to 0.2 K accuracy. The minimum spectral resolutions were 0.007, 0.010 and 0.011 Hz and 4, 8 and 8 transients were acquired (1 s relaxation delay) and added together for each 700, 500 and 400 MHz spectrum, respectively.

3.3. Elucidation of RDC from NMR Spectra and Experimental Errors

The experimental values of the methylene protons splitting $\Delta\nu$ were estimated from NMR spectra by: (i) fitting two Lorentzian line shapes and (ii) simulating with the SPINACH package the methylene resonance [57]. The least square method script written in the Matlab was used in both cases [58]. To minimize shimming errors more importance was placed to correctly map the spectral points which amplitude was above the amplitude at half-width than those whose amplitude was below. The starting fitting parameters were allowed to vary at the fixed range until converged. Spectra were simulated with SPINACH simulation package for Matlab using both formalism of the axial ordering matrix and an isotropic *J*-coupling between protons [57]. Due to the speed of simulation the simplified case of isotropic *J*-couplings was used to elucidate all splitting used in subsequent analyzes.

Two independent samples of zephycandidine in methanol-*d*₄, acetone-*d*₆ and chloroform-*d* were prepared and measured on all NMR instruments on the same day. These samples were also re-measured 6 months later to account for any instabilities related to the superconductive magnets of the spectrometer. Three to five spectra were recorded for each solution at 297 K, each following the same protocol, from which $\Delta\nu$ were extracted with the standard deviation of 0.015 Hz for 700 MHz spectrometer and 0.025 Hz for 500 and 400 MHz spectrometers. The standard deviation for the non-methylene $\Delta\nu$ was 0.015 Hz for all instruments.

The anisotropies of magnetic susceptibility ($\Delta\chi_{ax}$) were calculated from the fit (see Figure 2) of the experimental data (including point at 0 T) using the simplified Equation (2) and structural parameters collected in Table 2. That yielded the standard deviation of $0.03 \times 10^{-27} \text{ JT}^{-2}$. The final experimental error of $0.06 \times 10^{-27} \text{ JT}^{-2}$ (two times standard deviation; the confidence level 95.4%) for $\Delta\chi_{ax}$ was estimated from the methylene protons $\Delta\nu$.

For other protons the experimental $\Delta\chi_{ax}$ and $\Delta\chi_{rh}$ were estimated by extracting first coupling *D* (*D* < 0 in all cases) from the magnetic field dependence of *J* (see Figure 3) and then from the modified Equation (3):

$$\frac{-60\pi^2 r_{AB}^3 kT}{\mu_0 \gamma_A \gamma_B} D_{AB} = \left[\frac{3}{2} \Delta\chi_{rh} \cos 2\beta - \Delta\chi_{ax} \right] \quad (4)$$

The parameters r_{AB} and θ describing the mutual orientation of pairs of interacting protons in the molecule (see Figure 1) are collected in Table 2. The final experimental errors of $0.14 \times 10^{-27} \text{ JT}^{-2}$ and $0.12 \times 10^{-27} \text{ JT}^{-2}$ were estimated for $\Delta\chi_{ax}$ and $\Delta\chi_{rh}$, respectively.

Table 2. The structural parameters used to elucidate magnetic anisotropy data.

Protons Interacting	$r_{AB}/\text{\AA}$	θ/deg
methylene	1.81	-
H ₂ -H ₁	2.45	0
H ₂ -H ₃	2.51	60
H ₂ -H ₄	4.18	90
H ₃ -H ₄	2.47	30
H ₃ -H ₁	4.17	120
H ₁₂ -H ₁₁	2.76	144

3.4. Magnetic Susceptibilities and Cohesion Energy Densities of the Solvents

The values of magnetic susceptibility (χ_{sol}) of deuterated solvents in air at normal pressure were taken from reference [38] with exception of acetic acid- d_6 for which the protonated value from [59,60] was assumed in the absence of the value for its deuterated form and ethanol- d_6 which was taken from [61]. Supplementary Material Table S1 lists all these values explicitly as well as molar volumes, boiling points, refractive indexes, dielectric constants, and dipole moments for both deuterated and protonated solvents used [62,63]. The values used to calculate the ratio pV_m^{-1} (electric dipole moment to molar volume) and $n_D V_m^{-1}$ (refractive index to molar volume) in Figure 5a,b, respectively, are also explicitly highlighted in Table S1.

The experimental cohesion energy densities ($\text{ced}/\text{Jcm}^{-3}$) taken from reference [39] were used in Figure 4, whereas empirical ced and ced polar, dispersion and hydrogen bond components were calculated as cube of the Hansen Solubility Parameters from the Appendix 1 in the reference [48]. The differences between these values (calculated for protonated solvents) were assumed to correctly reflect the values for their deuterated versions in the absence of ced's data for the later. Supplementary Material Table S2 also lists for comparison, other experimental and averaged values of ced reported in [33,39,43–45,48]. Supplementary Material Table S3 compares values of ced for acetic acid from several sources [39,43,46–48].

3.5. Details of the Energy Barrier Evaluation

The energy barrier ΔE was estimated as a difference between the activation energies calculated from the predicted and experimentally measured temperature variations of the $\Delta\nu$ at 16.445 T (Figure 5b).

The previously evaluated magnetic anisotropy $\Delta\chi_{ax}$ of each solvent (Table 1) was used to calculate the predicted values of $\Delta\nu$ (from Equation (2) in Section 3.1) at the same temperatures the NMR spectra were recorded. Then, the Arrhenius plot was created for the natural logarithm of the predicted splitting as a function of the inverse of the temperature (dotted lines in Figure 5b). The predicted activation energy was obtained using linear regression fit in Matlab [51].

The same fitting procedure was applied to the experimental variable temperature $\Delta\nu$ data to obtain experimental activation energy and the energy barrier ΔE was estimated as a difference between these two values. The experimental error for ΔE was estimated to be 0.28 kJ/mol.

In the Supplementary Material, the step-by-step description of the procedure above is also given.

4. Conclusions

The aromatic molecules of zephycandidine sense the external magnetic field and have a preferred orientation with respect to its direction. Therefore, they do not rotate freely in the solution but spend considerably more time at a preferred position. This re-introduces an anisotropic interaction and residual dipolar couplings (rdc) are clearly observed in the NMR spectra.

The contributions of the dipole–dipole D -coupling and the anisotropic J -coupling to the splitting $\Delta\nu$ of methylene resonance can be quantitatively distinguished because the molecular geometry of zephycandidine makes possible to observe rdc from both methylene protons and protons laying in the symmetry plane of the molecule.

The large anisotropy of the magnetic susceptibility $\Delta\chi_{ax}$ and proximity of interacting magnetic moments are responsible for unusually large value of $\Delta\nu$, and the influence of the diamagnetic surrounding of the solvent on the solute for several deuterated solvents and at the wide range of temperatures could be studied.

The absolute values of $\Delta\chi_{ax}$ are larger for protic solvents due to the presence of hydrogen bonds as compared to aprotic solvents for which polar and dispersion forces play more important role in modulating molecular dynamic. The energy barrier attributed to hydrogen bonding is estimated to be 1.22 kJ/mol for methanol- d_4 , 0.85 kJ/mol for ethanol- d_6 , and 0.87 kJ/mol for acetic acid- d_4 . For aprotic but highly polar dimethyl sulfoxide- d_6 , the energy barrier of 1.08 kJ/mol corresponds to the direct interaction of the solvent lone pair electrons with π -electrons of zephycandidine. The energy barrier decreases for acetone- d_6 to 0.33 kJ/mol as its electric dipole moment is smaller than that for dimethyl sulfoxide- d_6 and for tetrahydrofuran- d_8 is below the experimental error of 0.28 kJ/mol. For acetonitrile- d_3 no energy barrier has been detected despite its electric dipole moment being comparable to that of dimethyl sulfoxide- d_6 . This is consistent with stronger solvent-solvent compared to solute-solvent interaction and could suggest ordering of the solvent molecules around solute. As a result, the fast reorientation of zephycandidine in acetonitrile- d_3 , cause the small absolute value of $\Delta\chi_{ax}$.

The largest absolute values of $\Delta\chi_{ax}$ are observed for zephycandidine dissolved in aromatic benzene- d_6 and toluene- d_8 which have their own preferential orientation at the external magnetic field and may enhance the order in the solution-solute system by as much as 15%.

The experimental cohesion energy density (ced) could be correlated with the changes in the anisotropy of magnetic susceptibility observed for both protic and aprotic solvents and that allows for the first time to approximate the value of $\Delta\chi_{ax}$ for an “isolated” zephycandidine molecule, not influenced by the solvent, to be $1.41 \times 10^{-27} \text{ JT}^{-2}$.

Supplementary Materials: The supporting information can be downloaded at: <https://www.mdpi.com/article/10.3390/ijms232315118/s1>.

Author Contributions: Synthesis of zephycandidine, J.T.-H. and P.J.M.; Methodology, experiments, analyses, and writing, R.M.K. All authors have read and agreed to the published version of the manuscript.

Funding: This research received no external funding.

Institutional Review Board Statement: Not applicable.

Informed Consent Statement: Not applicable.

Data Availability Statement: The data that support the findings of this study are available from the corresponding author upon reasonable request.

Acknowledgments: Chemical Analysis Facility at the University of Reading is thanked for providing access to NMR instrumentation. Author thanks G. D. Brown for the constructive criticism and support with experiments. University of Reading and CAF are thanked for making it possible to publish this work as an open access resource.

Conflicts of Interest: The authors declare no conflict of interest.

References

1. Li, G.W.; Liu, H.; Qiu, F.; Wang, X.J.; Lei, X.X. Residual dipolar couplings in structure determination of natural products. *Nat. Prod. Bioprospecting* **2018**, *8*, 279–295. [CrossRef]
2. Boettcher, B.; Thiele, C.M. Determining the stereochemistry of molecules from residual dipolar couplings (RDCs). *eMagRes* **2012**, *1*, 169–180.

3. Chen, K.; Tjandra, N. The use of residual dipolar coupling in studying proteins by NMR. *Top. Curr. Chem.* **2012**, *326*, 47–68. [[PubMed](#)]
4. Prestegard, J.H.; Bougault, C.M.; Kishore, A.I. Residual dipolar couplings in structure determinations of biomolecules. *Chem. Rev.* **2004**, *104*, 3519–3540. [[CrossRef](#)] [[PubMed](#)]
5. Kramer, F.; Deshmukh, M.V.; Kessler, H.; Glaser, S.J. Residual dipolar coupling constants: An elementary derivation of key equations. *Concepts Magn. Reson. Part A* **2004**, *21*, 10–21. [[CrossRef](#)]
6. Bertini, I.; Luchinat, C.; Parigi, G.; Ravera, E. The effect of partial orientation: Residual dipolar couplings. In *NMR of Para-Magnetic Molecules*, 2nd ed.; Elsevier: Amsterdam, The Netherlands, 2016; pp. 61–67.
7. Lei, X.; Sun, H.; Bai, L.; Wang, W.X.; Xiang, W.; Xiao, H. A self-assembled oligopeptide as a versatile NMR alignment medium for the measurements of residual dipolar couplings in methanol. *Angew. Chem. Int. Ed.* **2017**, *56*, 12857–12861. [[CrossRef](#)]
8. Naumann, C.; Kuchel, P.W. Prochiral and chiral resolution in ^2H NMR spectra: Solutes in stretched and compressed gelatin gels. *J. Phys. Chem. A* **2008**, *112*, 8659–8664. [[CrossRef](#)]
9. Kummerlöwe, G.; Halbach, F.; Laufer, B.; Luy, B. Precise measurement of RDCs in water and DMSO based gels using a silicone rubber tube for tunable stretching. *Open Spectrosc. J.* **2008**, *2*, 29–33. [[CrossRef](#)]
10. Emsley, J.W.; Rauzah, H.; Luckhurst, G.R.; Rumbles, G.N.; Vioria, F.R. The Saupe ordering matrices for solutes in uniaxial liquid crystals. Experiment and theory. *Mol. Phys.* **1983**, *6*, 1321–1335. [[CrossRef](#)]
11. Buckingham, A.D. Angular correlation in liquids. *Discuss. Faraday Soc.* **1967**, *43*, 205–211. [[CrossRef](#)]
12. Saupe, A. Kernresonanzen in kristallinen Flüssigkeiten und in kristallin-flüssigen lösungen. *Z. Naturforsch.* **1964**, *19*, 161–171. [[CrossRef](#)]
13. Anet, F.A.L. Magnetic alignment in the 500 MHz ^1H NMR spectrum of o-dichlorobenzene in acetone- d_6 . *J. Am. Chem. Soc.* **1986**, *108*, 1354–1355. [[CrossRef](#)]
14. Lisicki, M.A.; Mishra, P.K.; Bothner-By, A.A.; Lindsey, J.S. Solution conformation of a porphyrin-quinone cage molecule determined by dipolar magnetic field effects in ultra-high-field NMR. *J. Phys. Chem.* **1988**, *92*, 3400–3403. [[CrossRef](#)]
15. Laatikainen, R.; Ratilainen, J.; Sebastian, R.; Santa, H. NMR study of aromatic-aromatic interactions for benzene and some other fundamental aromatic systems using alignment of aromatics in strong magnetic field. *J. Am. Chem. Soc.* **1995**, *117*, 11006–11010. [[CrossRef](#)]
16. Heist, L.M.; Poon, C.-D.; Samulski, E.T.; Photinos, D.J.; Jokisaari, J.; Vaara, J.; Emsley, J.W.; Mamone, S.; Lelli, M. Benzene at 1 GHz. Magnetic field-induced fine structure. *J. Magn. Reson.* **2015**, *258*, 17–24. [[CrossRef](#)]
17. Karschin, N.; Wolkenstein, K.; Griesinger, C. Magnetically induced alignment of natural products for stereochemical structure determination via NMR. *Angew. Chem. Int. Ed.* **2020**, *59*, 15860–15864. [[CrossRef](#)]
18. Van Zijl, P.C.M.; Ruessink, B.H.; Bulthuis, J.; MacLean, C. NMR of partially aligned liquids: Magnetic susceptibility anisotropies and dielectric properties. *Acc. Chem. Res.* **1984**, *17*, 172–180. [[CrossRef](#)]
19. Shestakova, A.K.; Makarkina, A.V.; Smirnova, O.V.; Shtern, M.M.; Chertkov, V.A. Orientation of molecules by magnetic field as a new source of information on their structures. *Russ. Chem. Bull.* **2006**, *55*, 1359–1367. [[CrossRef](#)]
20. Jokisaari, J.; Kantola, A.M.; Vaara, J. Magnetic field-induced effects on NMR properties. *J. Magn. Reson.* **2017**, *281*, 1–6. [[CrossRef](#)]
21. Dracinsky, M.; Boul, P.J. Computational analysis of solvent effects in NMR spectroscopy. *Chem. Theory Comput.* **2010**, *6*, 288–299. [[CrossRef](#)]
22. Zhan, G.; Qu, X.; Liu, J.; Tong, Q.; Zhou, Q.; Sun, B.; Yao, G. Zephycandidine A, the first naturally occurring imidazo[1,2-f]phenanthridine alkaloid from *Zephyranthes candida*, exhibits significant anti-tumor and anti-acetylcholinesterase activities. *Sci. Rep.* **2016**, *6*, 33990. [[CrossRef](#)]
23. Murphy, P.J.; Tibble-Howlings, J.; Kowalczyk, R.M.; Stevens, K. Synthesis of zephycandidine A from haemanthamine. *Tetrahedron Lett.* **2020**, *61*, 151785. [[CrossRef](#)]
24. Sheng, B.; Zeng, C.; Chen, J.; Ye, W.-C.; Tang, W.; Lan, P.; Banwell, M.G. Total syntheses of the imidazo[1,2-f]phenanthridine containing alkaloid Zephycandidine A. *Eur. J. Org. Chem.* **2022**, *2022*, e202101511. [[CrossRef](#)]
25. Whitesides, G.M.; Holtz, D.; Roberts, J.D. Nuclear Magnetic Resonance Spectroscopy. The effect of structure on magnetic nonequivalence due to molecular asymmetry. *J. Am. Chem. Soc.* **1964**, *86*, 2628–2634. [[CrossRef](#)]
26. Ault, A. Classification of spin systems in NMR spectroscopy. *J. Chem. Educ.* **1970**, *47*, 812–818. [[CrossRef](#)]
27. Petrakis, L. Spectra line shapes. Gaussian and Lorentzian functions in magnetic resonance. *J. Chem. Educ.* **1967**, *44*, 432–436. [[CrossRef](#)]
28. Zerbe, O.; Jurt, S. *Applied NMR Spectroscopy for Chemists and Life Scientists*; Wiley: Weinheim, Germany, 2014; pp. 17–20.
29. Levitt, M.H. *Spin Dynamics*, 2nd ed.; Wiley: Chichester, UK, 2015; pp. 51, 211–223.
30. Johannesen, R.B.; Feretti, J.A.; Harris, R.K. UEAIR: A new computer program for analysis of NMR spectra analysis of the proton spectrum of triisopropylphosphine. *J. Magn. Reson.* **1970**, *3*, 84–93. [[CrossRef](#)]
31. Vaara, J.; Jokisaari, J.; Wasylishen, R.E.; Bryce, D.L. Spin-spin coupling tensors as determined by experiment and computational chemistry. *Nucl. Magn. Reson. Spectrosc.* **2002**, *41*, 233–304. [[CrossRef](#)]
32. Pauling, L. The diamagnetic anisotropy of aromatic molecules. *J. Chem. Phys.* **1936**, *4*, 673–677. [[CrossRef](#)]
33. Dack, M.R.J. The importance of solvent internal pressure and cohesion to solution phenomena. *Chem. Soc. Rev.* **1975**, *4*, 211–229. [[CrossRef](#)]

34. Marcus, Y. The properties of organic liquids that are relevant to their use as solvating solvents. *Chem. Soc. Rev.* **1993**, *6*, 409–416. [CrossRef]
35. Hoffman, R.E. Variations on the chemical shift of TMS. *J. Magn. Reson.* **2003**, *163*, 325–331. [CrossRef]
36. Hoffman, R.E.; Becker, E.D. Temperature dependence of the ^1H chemical shift of tetramethylsilane in chloroform, methanol and dimethylsulfoxide. *J. Magn. Reson.* **2005**, *176*, 87–98. [CrossRef]
37. Hoffman, R.E. Standardization of chemical shifts of TMS and solvent signals in NMR solvents. *Magn. Reson. Chem.* **2006**, *44*, 606–616. [CrossRef]
38. Hoffman, R.E. Magnetic susceptibility measurement by NMR: 2. The magnetic susceptibility of NMR solvents and their chemical shifts. *J. Magn. Reson.* **2022**, *335*, 107105. [CrossRef] [PubMed]
39. Barton, A.F.M. Solubility parameters. *Chem. Rev.* **1975**, *75*, 731–753. [CrossRef]
40. Pirika.com. Available online: <https://pirika.com/index.html> (accessed on 9 June 2022).
41. Faubel, M.; Kisters, T. Non-equilibrium molecular evaporation of carboxylic acid dimers. *Nature* **1989**, *339*, 527–529. [CrossRef]
42. Slavchov, R.I.; Novev, J.K.; Mosbach, S.; Kraft, M. Vapor Pressure and Heat of Vaporization of Molecules That Associate in the Gas Phase. *Ind. Eng. Chem. Res.* **2018**, *57*, 5722–5731. [CrossRef]
43. Belmares, M.; Blanco, M.; Goddard, W.A., III; Ross, R.B.; Caldwell, G.; Chou, S.-H.; Pham, J.; Olofson, P.M.; Thomas, C. Hildebrand and Hansen Solubility Parameters from Molecular dynamics with application to electronic nose polymer sensors. *J. Comput. Chem.* **2004**, *25*, 1814–1826. [CrossRef]
44. D’Amelia, R.P.; Tomic, J.C.; Nirode, W.F. The determination of the solubility parameter (δ) and the Mark-Houwink constants (K & α) of food grade polyvinyl acetate (PVAc). *J. Polym. Biopolym. Phys. Chem.* **2014**, *2*, 67–72.
45. Hübel, H.; Faux, D.A.; Jones, R.B.; Dunstan, D.J. Solvation pressure in chloroform. *J. Chem. Phys.* **2006**, *124*, 204506-1–204506-7. [CrossRef]
46. Konicek, J.; Wadsö, I. Enthalpies of vaporization of organic compounds. *Acta Chem. Scand.* **1970**, *24*, 2612–2616. [CrossRef]
47. Chickos, J.S.; Acree, W.E., Jr. Enthalpies of vaporization of organic and organometallic compounds 1880–2002. *J. Phys. Chem. Ref. Data* **2003**, *32*, 519–878. [CrossRef]
48. Hansen, C.M. *Hansen Solubility Parameters. A User’s Handbook*, 2nd ed.; CRC Press: London, UK; New York, NJ, USA, 2007; pp. 4–6, 13–17, 45–59.
49. Atkins, P.W. *Physical Chemistry*, 3rd ed.; Oxford University Press: Oxford, UK, 1986; pp. 584–586.
50. Takamuku, T.; Tabaya, M.; Yamaguchi, A.; Nishimoto, J.; Kumamoto, M.; Wakita, H.; Yamaguchi, T. Liquid structure of acetonitrile-water mixtures by x-ray diffraction and infrared spectroscopy. *J. Phys. Chem. B* **1998**, *102*, 8880–8888. [CrossRef]
51. Timerghazin, Q.K.; Peslherbe, G.H. Electronic structure of the acetonitrile and acetonitrile dimer anions: A topological investigation. *J. Phys. Chem. B* **2008**, *112*, 520–528. [CrossRef] [PubMed]
52. Ford, T.A.; Glasser, L. Ab initio calculations of the structural, energetic, and vibrational properties of some hydrogen bonded and van der Waals Dimers. Part 4. The acetonitrile dimer. *Int. J. Quantum Chem.* **2001**, *84*, 226–240. [CrossRef]
53. Siebers, J.G.; Buck, U.; Beu, T.A. Calculation of structures and vibrational spectra of acetonitrile clusters. *Chem. Phys.* **1998**, *239*, 549–560. [CrossRef]
54. Reimers, J.R.; Hall, L.E. The solvation of acetonitrile. *J. Am. Chem. Soc.* **1999**, *121*, 3730–3744. [CrossRef]
55. Vukovic, V.; Pitesa, T.; Jelsch, C.; Wenger, E.; Molcanov, K. An unusual intermolecular interaction between a lone pair and an electron-rich π electron system of a quinoid dianion. *Cryst. Growth Des.* **2021**, *21*, 5651–5658. [CrossRef]
56. Schottel, B.L.; Chifotides, H.T.; Dunbar, K.R. Anion- π interactions. *Chem. Soc. Rev.* **2008**, *37*, 68–83. [CrossRef]
57. Hogben, H.J.; Krzystyniak, M.; Charnock, G.T.P.; Hore, P.J.; Kuprov, I. Spinach—A software library for simulation of spin dynamics in large spin systems. *J. Magn. Reson.* **2011**, *208*, 179–194. [CrossRef] [PubMed]
58. MATLAB, version R2021a; The Mathworks, Inc.: Natick, MA, USA, 2021.
59. Deshpande, V.T.; Pathki, K.G. Magnetic susceptibility of acetic acid + pyridine mixtures. *Trans. Faraday Soc.* **1962**, *58*, 2134–2138. [CrossRef]
60. Sriraman, S.; Shanmugasundaram, V.; Sabesan, R. The diamagnetic study of the nature of the association of acetic acid. II. The binary systems of acetic acid with Triethylamine, pyridine and Aniline. *Bull. Chem. Soc. Jpn.* **1965**, *38*, 1391–1393. [CrossRef]
61. Available online: <https://nmr.chem.umn.edu/ResReports/NMR002.html> (accessed on 12 June 2022).
62. Christian Reichardt, C.; Welton, T. *Solvents and Solvent Effects in Organic Chemistry*, 4th ed.; Appendix A; Wiley: Weinheim, Germany, 2011; pp. 549–553.
63. *Bruker Almanac 2012*; Bruker Corporation: Billerica, MA, USA, 2012; NMR tables p15.